Extreme significant wave height of tropical cyclone waves in the South China Sea

Zhuxiao Shao[1], Bingchen Liang[1, 2], Huajun Li[1, 2], Ping Li[3], Dongyoung Lee[1, 4]

[1] College of Engineering, Ocean University of China, 238 Songling Road, Qingdao 266100, China

[2] Shandong Province Key Laboratory of Ocean Engineering, Ocean University of China, 238 Songling Road, Qingdao 266100, China

[3] China Classification Society, Beijing 100007, China

[4] Korea Institute of Ocean Science & Technology, Ansan, Korea

Corresponding to: Bingchen Liang (bingchen@ouc.edu.cn)

ABSTRACT

Extreme significant wave heights are assessed in the South China Sea (SCS), as assessments of wave heights are crucial for coastal and offshore engineering. Two significant factors include the initial database and assessment method. The initial database is a basis for assessment, and the assessment method is used to extrapolate appropriate return significant wave heights during a given period. In this study, a 40-year (1975-2014) hindcast of tropical cyclone waves is used to analyse the extreme significant wave height, employing the peak over threshold (POT) method with the generalized Pareto distribution (GPD) model. The peak excesses over a sufficiently large value (i.e., threshold) are fitted; thus, the return significant wave heights are highly dependent on the threshold. To determine a suitable threshold, the sensitivity of return significant wave heights and the characteristics of tropical cyclone waves are studied. The sample distribution presents a separation that distinguishes the high sample from the low sample, and this separation is within the stable threshold range. In addition, the asymptotic tail approximation and estimation uncertainty are reasonable based on the high sample value.

1. Introduction

Reasonable assessments of extreme significant wave heights are highly important for the security and expense of coastal defence and offshore structures (Ojeda and Guillén, 2006, 2008; Ojeda et al., 2010, 2011; Mortlock and Goodwin, 2015, 2016; Mortlock et al., 2017). To obtain this assessment, a sample is extracted from an accurate initial database, the extreme sample is identified by a reliable sampling method, and then, an appropriate probability distribution model is fitted.

The initial database highly influences the assessment of extreme significant wave heights (Godoi et al., 2017; Lucas et al., 2017; Li et al., 2018). In previous studies, the long-term continuous database is usually employed as the initial database, such as a 32-year measured significant wave height in the Gulf of Maine (Viselli et al., 2015), a 44-year hindcasted significant wave height in the North Atlantic Ocean (Muraleedharan et al., 2016) and a 22-year hindcasted significant wave height in the Yellow Sea (Gao et al., 2018). Considering that the extreme significant wave height should be extrapolated based on an independent and identically distributed database required for the extreme value theory (EVT) (Coles, 2001; Sobradelo et al., 2011), these time series buoy measurements and numerical hindcasts should be processed. The homogenous methodology is used to extract homogenous significant wave heights via separation in carefully chosen directional sectors and seasonal analyses as well as separation of the sea state into independent wave systems (Lerma et al., 2015; Solari and Alonso, 2017). Declustering methodology, such as the double-threshold approach (Mazas and Hamm, 2011) and minimum separation time method (Kapelonis et al., 2015), is used to differentiate the individual wave event. However, these methodologies may introduce uncertainty in the sample (such as the subjectivity of practitioners in the selections of initial threshold and time window), which influences the extreme sample selection.

The peak over threshold (POT) method (Goda et al., 2001) is widely used to identify the peak excesses over a threshold (Ferreira and Guedes Soares, 1998; Soares and Scotto, 2004; Caires and Sterl, 2005; Benetazzo et al., 2012; You and Callaghan, 2013; Xiao et al., 2017). Additionally, the generalized Pareto distribution (GPD) model (Coles, 2001) is widely used to extrapolate extreme significant wave heights (Martucci et al., 2010; Blanchet et al., 2015; Kapelonis et al., 2015; Boessenkool et al., 2017; Muhammed Naseef and Sanil Kumar, 2017). This method (i.e., the POT/GPD method) makes the most of the samples and extends the return period when the threshold is suitable (Alves and Young, 2003; You, 2011; Vanem, 2015a; Samayam et al., 2017; Shao et al., 2017). To select a suitable threshold, many methods have been proposed, such as graphical diagnostics (Coles, 2001; Sánchez-Arcilla et al., 2008; Bernardara et al., 2014), empirical methods (Ferreira et al., 2003; Neves and Alves, 2004; Reiss and Thomas, 2007), probabilistic-based techniques (Hill, 1975; Beirlant et al., 2006; Goegebeur et al., 2008), computational approaches (Danielsson et al., 2001; Beguería, 2005; Solari et al., 2017) and mixture models (Carreau and Bengio, 2009; Eastoe and Tawn, 2010; MacDonald et al., 2011). Among these methods, a graphical diagnostic referred to as the sensitivity of the return significant wave height to the threshold (Scarrott and MacDonald, 2012) is commonly accepted (Petrov et al., 2013; Northrop and Coleman, 2014; Vanem, 2015b; Northrop et al., 2017; Sulis et al., 2017).

In the South China Sea (SCS), time series wave parameters have been simulated (Zheng et al., 2012; Mirzaei et al., 2015; Yaakob et al., 2016), and extreme waves have been investigated based on long-term continuous data (Zheng et al., 2015; Chen et al., 2017; Wang et al., 2018). In addition, Shao et al. (2018a) and Liang et al. (2019) analysed the extreme significant wave height in a tropical cyclone. Shao et al. (2018a) compared the annual maxima (AM) method (Tawn, 1988) with the POT method. The AM method is an easy sampling method that does not require additional work, as the method directly extracts the annual maximal significant wave height for extrapolation. However, the AM method has limitations in a fixed time window (i.e., one year), which cannot guarantee the independence and number of samples. The annual maximal significant wave height obtained from neighbouring years may originate from the same extreme wave; some maximal significant wave heights may be neglected (i.e., the annual maximal significant wave height may be smaller than some unselected maximal significant wave heights in other years), resulting in an insufficient number of samples, especially for a relatively long return period. In a tropical cyclone, the AM method's limitation is further exacerbated, even if the return period is close to the database size. The annual frequency, intensity and track of recorded tropical cyclones greatly vary, and corresponding waves have obvious differences. Shao et al. (2018a) found that the minimal sample may be much less than the maximal sample, and the minimal sample may be too small to represent the extreme wave (i.e., the minimal sample in the AM method is obviously smaller than the extreme sample in the POT method). Compared with the AM method, the POT method is a natural sampling method without additional limitations. When the threshold is suitable, the POT method can guarantee the representativeness and number of extreme samples. However, the threshold selection process is relatively complex. Shao et al. (2018a) and Liang et al. (2019) analysed the sensitivity of the return significant wave height to the threshold. The researchers found that the suitable threshold should be determined within the stable threshold range (i.e., a threshold range corresponding to a range of stable return significant wave heights). Based on this conclusion, Shao et al. (2018a) defined the largest threshold within the common stable threshold range as the suitable threshold, and Liang et al. (2019) proposed an Automated Threshold Selection Method based on the characteristic of Extrapolated significant wave heights (the acronym is ATSME). The ATSME employs the differences in extrapolated significant wave heights for neighbouring thresholds as the diagnostic parameters to identify the uniquely stable threshold range via an automated method and selects the largest threshold within the stable threshold range as the suitable threshold for different return periods.

In this study, the assessment of extreme significant wave heights is further studied in the SCS. Before the assessment, the meteorological characteristics are analysed to identify extreme weather. In the SCS, the tropical cyclone always drives the storm wave (Anoop et al., 2015; Hithin et al., 2015; Sanil Kumar and Anoop, 2015; Ojeda et al., 2017; Wang et al., 2017; Mortlock et al., 2018; Sanil Kumar et al., 2018), and the number of tropical cyclones is sufficiently large. Thus, it is possible to study the extreme significant wave height in a tropical cyclone. To achieve the assessment, a 40-year (1975-2014) hindcasted significant wave height of tropical cyclone waves is employed as the initial database. Considering that the hindcast is independently simulated during the tropical cyclone recorded in the SCS, the maximal significant wave height of the tropical cyclone wave can be directly extracted as the sample when the tropical cyclone influences the wave at the targeted location. Based on the sample, the POT method threshold is studied. By analysing the sensitivity of the return significant wave heights and the characteristics of the tropical cyclone waves, the sample distribution presents a separation within the stable threshold range. As validated by the asymptotic tail approximation and estimation uncertainty, the high sample shown in the distribution of the sample is suitable for extrapolating extreme significant wave heights in the SCS.

The article is structured as follows. In the next section, the POT/GPD and ATSME are introduced. The initial data and study sites are presented in Section 3. In Section 4, the sampling method is described. In Section 5, the characteristics of tropical cyclone waves are discussed. Finally, the conclusions and discussions are presented in Section 6.

2. Background

2.1 POT/GPD

The POT method extracts the maximal significant wave heights above a selected value (i.e., threshold), u, as the extreme sample. For u, which is sufficiently large, the distribution function of peak excesses can be approximated by a member of the GPD (Pickands, 1975; Embrechts et al., 1997):

$$F_u\left(Hs^*\right)=\begin{cases}1-(1+k\dfrac{Hs^*}{\sigma})^{-\frac{1}{k}} & k\neq 0\\ 1-\exp\left(-\dfrac{Hs^*}{\sigma}\right) & k=0\end{cases} \tag{1}$$

where Hs^* represents the peak excess over the threshold; σ represents the scale parameter; and k represents the shape parameter. These GPD parameters (σ and k) are estimated using the maximum likelihood estimation method, which is recommended by Mazas and Hamm (2011):

$$\ln L(k,\sigma;Hs)=\begin{cases}-N\ln\sigma+(\dfrac{1}{k}-1)\sum_{j=1}^{N}\ln(1-\dfrac{kHs_j}{\sigma}) & k\neq 0\\ -N\ln\sigma-\dfrac{1}{\sigma}\sum_{j=1}^{N}Hs_j, & k=0\end{cases} \tag{2}$$

where N represents the number of events exceeding the threshold (i.e., the number of extreme samples), and Hs represents the maximal significant wave height.

The return significant wave height for the i-year, Hs_i, is defined as follows:

$$Hs_i = F_u^{-1}(1-\frac{1}{i}) \tag{3}$$

Thus, the value can be calculated with the following equation:

$$Hs_i = \begin{cases} u + [(\frac{N}{N_T}i)^k - 1]\sigma / k & k \neq 0 \\ u + \sigma \ln(\frac{N}{N_T}i) & k = 0 \end{cases} \tag{4}$$

where N_T represents the size of the dataset.

2.2 ATSME

The terms $u_1,\ldots, u_m$ are equally spaced with increasing candidate thresholds. $Hs_{i,j}$ represents the return significant wave height for the i-year based on the threshold of u_j. The difference, $\Delta Hs_{i,j}$, in i-year return significant wave heights ($Hs_{i,j}$ and $Hs_{i,j-1}$) for neighbouring thresholds (u_j and u_{j-1}) is defined as follows:

$$\Delta Hs_{i,j} = Hs_{i,j} - Hs_{i,j-1} \tag{5}$$

To study the influence of the excluded samples on the return significant wave height with an increasing threshold and to select a suitable threshold, the ATSME is defined as follows (Liang et al., 2019):

(1) Sample. Take the sample from the initial database under an independent and identically distributed assumption.

(2) Candidate threshold. Identify the suitable range for the equally spaced and increasing candidate thresholds, (u_1, u_m), and the threshold interval, $\Delta u = \frac{u_m - u_1}{N_{tot}}$. u_1 is set as the minimal sample, u_m is set as the maximal sample, and N_{tot} is set as the number of samples.

(3) Return period and value. Choose the order of i ($i = i_1, ..., i_{n_i}$) for different return periods, which is dependent on N_T and the requirement of practitioners. Extrapolate the return significant wave height for the i-year, $Hs_{i,j}$, which corresponds to every candidate threshold, u_j.

(4) Stable threshold range. Calculate the difference, $\Delta Hs_{i,j}$, in the return significant wave height for neighbouring thresholds. Define a characteristic parameter, $ch_{i,j}$, to record the stable characteristics of the return significant wave heights. Find the uniquely stable threshold range for the i-year return period.

(5) Suitable threshold. Determine the suitable threshold within the stable threshold range, such as the maximal threshold.

By the ATSME, a unique threshold is determined within a uniquely stable threshold range for a specific return period. Liang et al. (2019) found that the stable threshold range shows a pattern associated with the return period. The minimal threshold of the stable threshold range controls the representativeness of the extreme sample; thus, the samples over the minimal threshold can represent extreme waves well, and the minimal thresholds for different return periods remain constant. The maximal threshold of the stable threshold range controls the number of extreme samples, and a longer return period requires more extreme samples; thus, the maximal thresholds gradually decrease when the return period increases. Consequently, excluding the sample within the stable threshold ranges does not obviously influence the return significant wave heights, and a suitable threshold should be determined within the stable threshold range.

3. Initial data and study sites

3.1 Initial data

Significant wave heights from a 40-year hindcast of tropical cyclone waves (Shao et al., 2018a) are adopted as the initial database, which is simulated using the third-generation spectral wind-wave model SWAN (an acronym for Simulating WAves Nearshore) (Booij et al., 1999; Mortlock et al., 2014; Amrutha et al., 2016). This model is forced by the blended wind, which is obtained by combining the European Centre for Medium-Range Weather Forecasts reanalysis wind and Holland model wind (Shao et al., 2018b). The spatial resolution is 0.0625° for both longitude and latitude, and the temporal resolution is 1 h. From 1975 to 2014, waves are simulated only during 974 independent tropical cyclones.

3.2 Study sites

To analyse the extreme significant wave height, 22 locations were selected as the study sites (Fig. 1). When the distance between the centre of the tropical cyclone and the study site is within 300 km, hourly significant wave heights simulated during this tropical cyclone are adopted as the initial database at the study site. At the 22 study sites, the number of recorded tropical cyclones is 247 to 403, and the annual mean number of recorded tropical cyclones is 6.175 to 10.075. The corresponding tropical cyclone waves are sufficient for assessing extreme significant wave heights in the SCS (Mazas and Hamm, 2011).

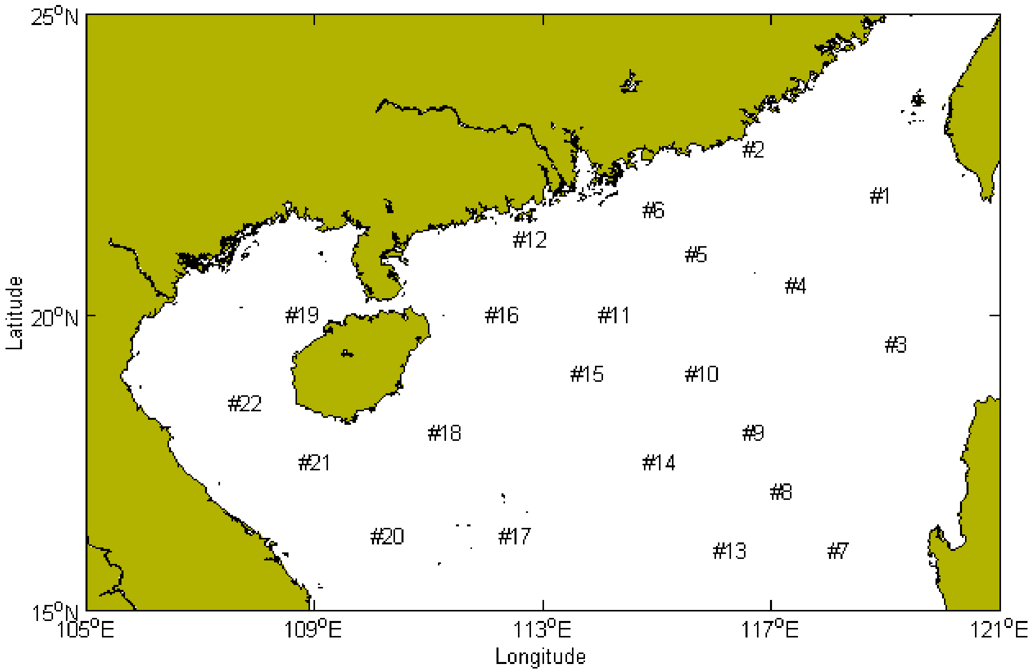

Fig. 1. The study sites in the study region.

4. Study of the POT method

4.1 Sample

As required by the EVT, the extreme significant wave height should be extrapolated based on the independent wave under the same type of meteorological event (Lerma et al., 2015; Solari and Alonso, 2017). Considering that the initial database is simulated only during the independent tropical cyclone, the maximal significant wave height of recorded tropical cyclone waves can be directly extracted as the sample at the study site. For example, 328 tropical cyclones are recorded at location #1; thus, 328 maximal significant wave heights during these tropical cyclones are extracted as the sample.

4.2 Sensitivity of return values to threshold

Sensitivity of the return significant wave height to the threshold can be used in threshold selection. This method fits the GPD over a range of candidate thresholds and selects the suitable threshold by identifying the stability of the return significant wave heights. If return significant wave heights are insensitive to the threshold, the corresponding threshold can be selected as the suitable threshold. The benefit of this method is that it requires practitioners to graphically inspect and comprehend the data features and assess the uncertainty of the candidate thresholds (Scarrott and MacDonald, 2012). The drawback of this method is that the threshold is not uniquely selected, and another criterion is needed to identify the optimal threshold (Lerma et al., 2015).

Shao et al. (2018a) and Liang et al. (2019) analysed the sensitivity of the return significant wave height and provided threshold selection criteria to determine a unique threshold. Liang et al. (2019) diagnosed the return significant wave height within the stable threshold range. If some return significant wave heights within the stable threshold range are relatively different from the others, the corresponding candidate thresholds are rejected. Thus, the conclusions of Liang et al. (2019) on the sensitivity of the return significant wave height are employed in this study. For example, at location #1, the equally spaced with increasing candidate thresholds are identified by a threshold interval of 0.05 m, and the stable threshold ranges for the 50-year, 100-year, 150-year and 200-year return periods are (3.3 m, 5.75 m), (3.3 m, 5.25 m), (3.3 m, 4.6 m) and (3.3 m, 4.5 m), respectively.

5. Characteristics of tropical cyclone waves

To further analyse the candidate thresholds within the stable threshold range, the characteristics of tropical cyclone waves are investigated. The track and intensity of tropical cyclones affect the waves at the study site. When the tropical cyclone track is close to the study site and the intensity of the tropical cyclone is strong, the corresponding wave is sufficiently strong for representing the extreme wave at the study site. In this case, the maximal significant wave height of this tropical cyclone wave should be extracted as the extreme sample. For example, at location #1, the maximal significant wave heights during tropical cyclones Pabuk in 2007, Linfa in 2009, Molave in 2009 and Meranti in 2010 are 5.27 m, 8.17 m, 9.48 m and 4.51 m, respectively. The tracks of these tropical cyclones are close to location #1, and the intensities of these tropical cyclones are strong when they influence the waves at location #1 (shown in Fig. 2).

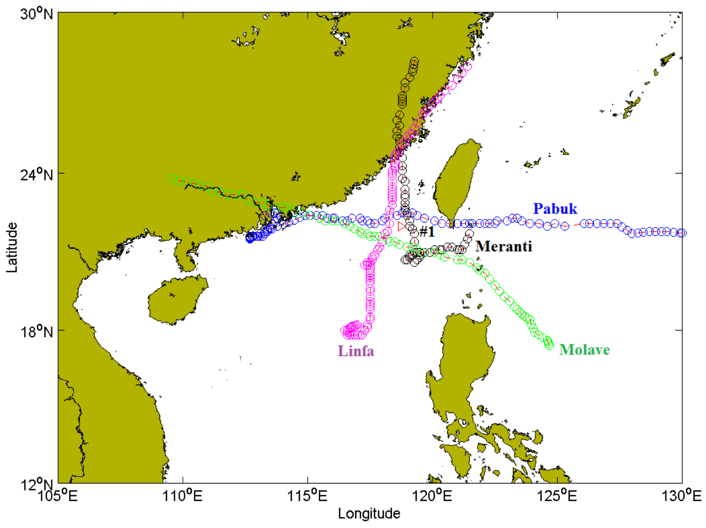

Fig. 2. Tracks of the centres of tropical cyclones Pabuk, Linfa, Molave and Meranti (triangle represents location #1, curves represent tracks of centres and circles represent locations of centres).

In contrast, when the track of the tropical cyclone is far from the study site or the intensity of the tropical cyclone is weak, the corresponding wave is insufficiently strong to represent the extreme wave at the study site. In this case, the maximal significant wave height of this tropical cyclone wave should not be extracted as the extreme sample. For example, at location #1, the maximal significant wave heights during tropical cyclones Maria in 2000 and Toraji in 2001 are 2.59 m and 1.57 m, respectively. Although the intensities of these tropical cyclones are strong when they influence the waves at location #1, the tracks of these tropical cyclones are too far from location

#1 (shown in Fig. 3). The maximal significant wave heights during tropical cyclones Trami in 2001 and Wutip in 2007 are 2.47 m and 2.20 m, respectively. Although the tracks of these tropical cyclones are close to location #1, the intensities of these tropical cyclones are weak when these tropical cyclones influence the waves at location #1 (shown in Fig. 4). The maximal significant wave heights during tropical cyclones Kai-tak in 2005 and Kammuri in 2008 are 1.11 m and 2.36 m, respectively. The tracks of these tropical cyclones are far from location #1, and the intensities of these tropical cyclones are weak when they influence the waves at location #1 (shown in Fig. 5).

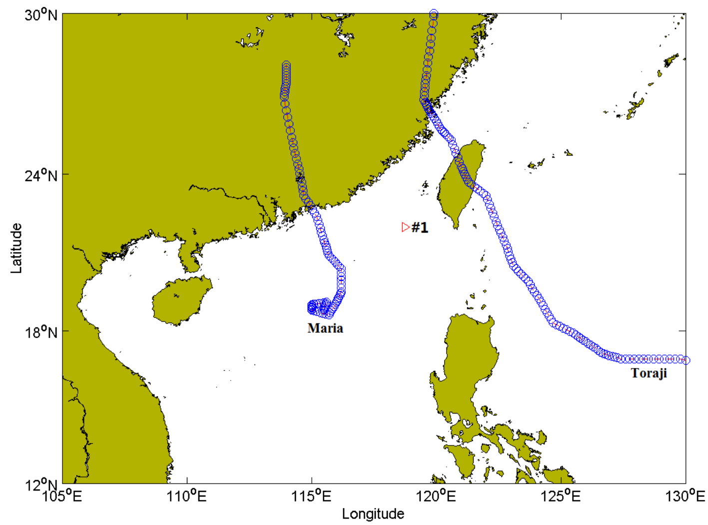

Fig. 3. Tracks of the centres of tropical cyclones Maria and Toraji (triangle represents location #1, curves represent tracks of centres and circles represent locations of centres).

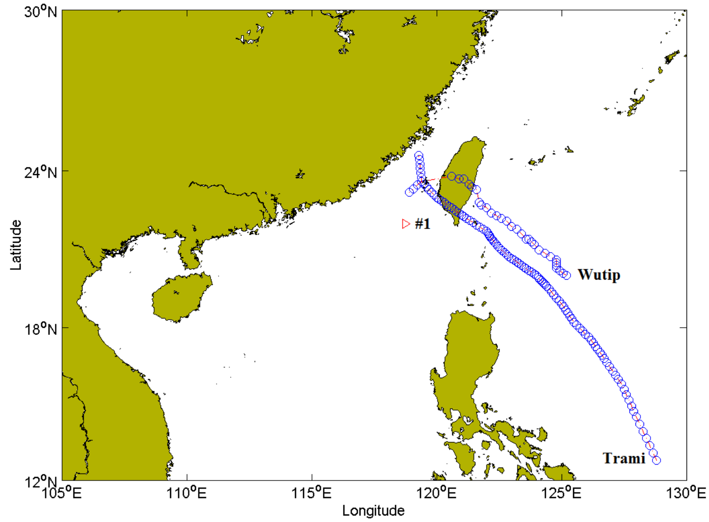

Fig. 4. Tracks of the centres of tropical cyclones Trami and Wutip (triangle represents location #1, curves represent tracks of centres and circles represent locations of centres).

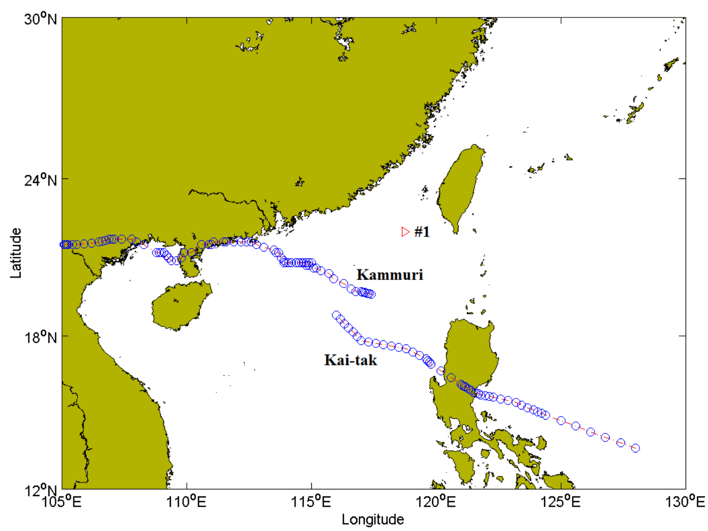

Fig. 5. Tracks of the centres of tropical cyclones Kai-tak and Kammuri (triangle represents location #1, curves represent tracks of centres and circles represent locations of centres).

The track and intensity influences of the tropical cyclones are reflected in the sample distribution (i.e., the distribution of the maximal significant wave height). In Fig. 6, the distribution of the sample at location #1 is presented. The sample is counted from 0 m to 15 m with an interval of 0.05 m, which is the same as the threshold interval. The samples are concentrated in two ranges: range 1 (0-4.15 m) and range 2 (4.15-15 m), with a separation value of 4.15 m (the curve is plotted to clearly show these ranges). In range 1, 191 samples from 191 independent tropical cyclone waves are found. The corresponding tropical cyclone has a weak influence on the wave at location #1, and its track and intensity are similar to those shown in Figs. 3, 4 and 5. In range 2, 137 samples from 137 independent tropical cyclone waves are found. The corresponding tropical cyclone has a strong influence on the wave at location #1, and its track and intensity are similar to those shown in Fig. 2. The sample distribution has a natural separation, distinguishing the high sample from the low sample. Linking the distribution with the sensitivity of the return significant wave height, this separation (the corresponding annual mean number of extreme samples is 3.425) is within the stable threshold range shown in subsection 4.2.

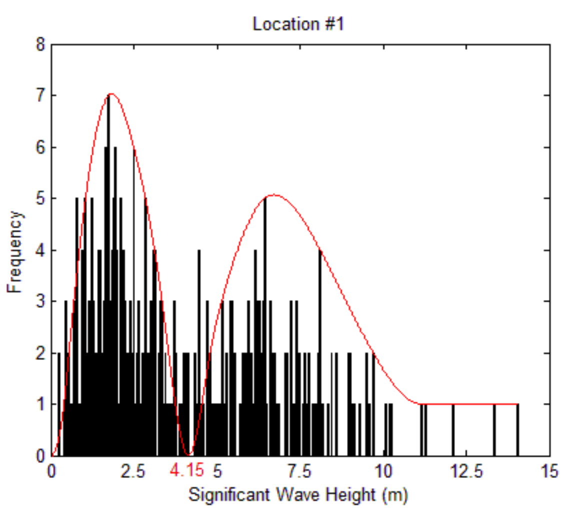

Fig. 6. Histogram of the maximal significant wave height from 0 m to 15 m with intervals of 0.05 m at location #1.

To further validate the separation, the asymptotic tail approximation and estimation uncertainty are analysed. The asymptotic tail approximation can be estimated by the quantile plot, which is discussed by Coles (2001) and produced by a free package running in R. In Fig. 7, the quantile plot for the threshold of 4.15 m is presented, which shows that there are generally few differences between the empirical and fitted quantiles, indicating a good fit for the selected threshold. In Table 1, the return significant wave height with the confidence interval is shown. The likelihood method (Schendel and Thongwichian, 2017) reparametrizes the likelihood in terms of the unknown quantile and uses profile likelihood arguments to construct an approximate 95% confidence interval. At location #1, the confidence intervals indicate that the variance in the extrapolated significant wave heights is acceptable.

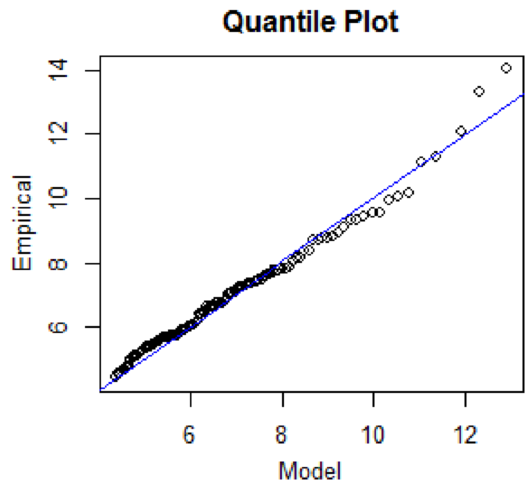

Fig. 7. The quantile plot for GPD-fitted maximal significant wave heights at location #1 for the threshold of 4.15 m.

Table 1
Statistics for the return significant wave heights and confidence intervals at location #1 for the threshold of 4.15 m.

Return Period	Return Significant Wave Height (m)	Confidence Interval (m)	Width of Confidence Interval (m)
50-year	12.07	(11.39, 13.08)	1.69
100-year	12.70	(12.02, 13.92)	1.90
150-year	13.00	(12.31, 14.36)	2.05
200-year	13.20	(12.50, 14.66)	2.16

The same conclusion can be reached at the other 21 study sites. For example, the sample distributions at locations #7 and #10 (Fig. 8) present separation values of 3.35 m and 4.1 m, respectively. Based on these separation values, the GPD model is used to extrapolate the return significant wave heights for return periods of 50-year, 100-year, 150-year and 200-year (Table 2). To validate the reliability of the return significant wave heights, the asymptotic tail approximation and estimation uncertainty are analysed. For example, the quantile plots at locations #7 and #10 are presented in Fig. 9, and the confidence intervals at 21 study sites are shown in Table 2. The fits of the results are good, and the uncertainties of the return significant wave heights are acceptable.

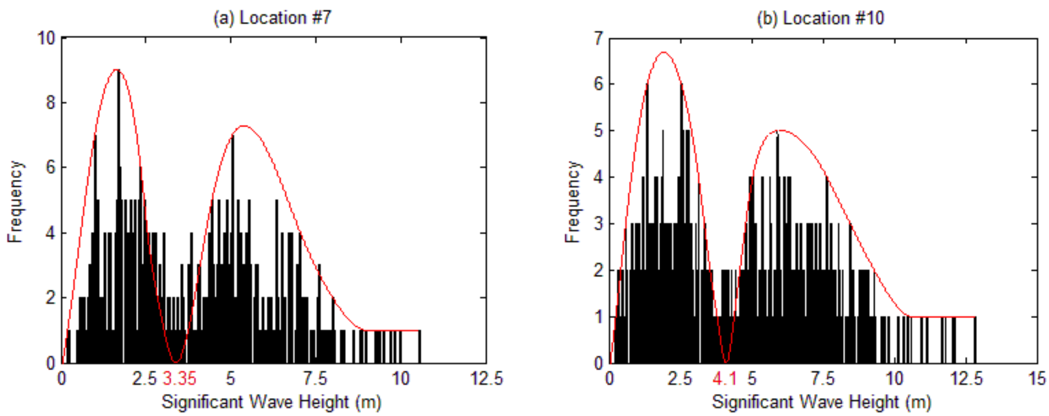

Fig. 8. Histograms of the maximal significant wave heights at locations #7 and #10.

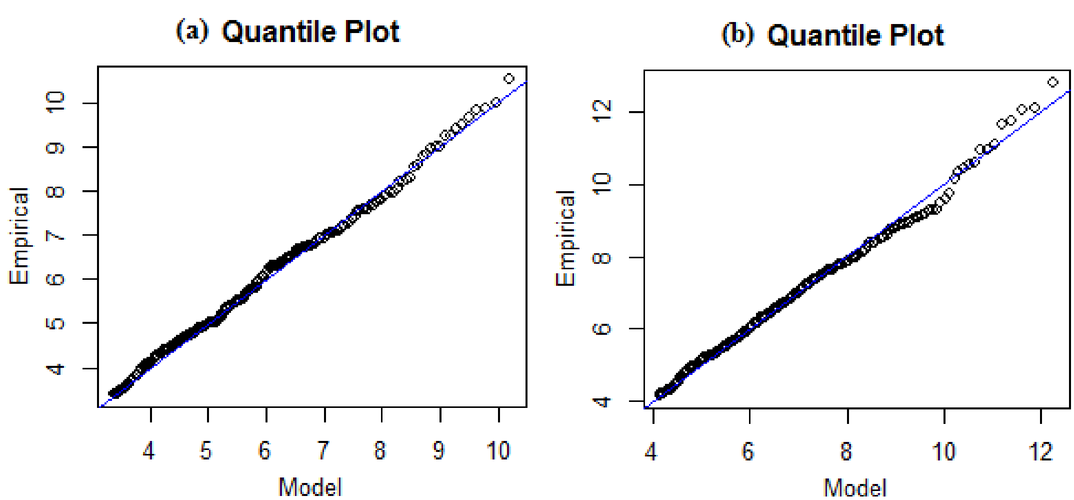

Fig. 9. Quantile plots for GPD-fitted maximal significant wave heights: (a) for the threshold of 3.35 m at location #7 and (b) for the threshold of 4.1 m at location #10.

Table 2
Statistics for thresholds, extreme samples and return significant wave heights with 95% confidence intervals.

Location	Threshold (m)	Annual Mean Number of Extreme Samples	Return Significant Wave Heights (m) with 95% Confidence Intervals			
			50-year	100-year	150-year	200-year
#2	3.05	3.475	9.25 (8.88, 9.88)	9.58 (9.19, 10.45)	9.74 (9.37, 10.74)	9.86 (9.46, 10.92)
#3	5	3.375	11.17 (10.74, 11.89)	11.45 (11.02, 12.34)	11.61 (11.18, 12.60)	11.71 (11.29, 12.78)
#4	4.85	4.175	12.00 (11.25, 12.91)	12.24 (11.65, 13.26)	12.52 (11.93, 13.66)	12.70 (12.09, 13.94)
#5	4.95	3.975	11.84 (11.17, 12.80)	12.53 (11.81, 13.74)	12.83 (12.13, 14.25)	13.06 (12.34, 14.61)
#6	4.5	3.625	10.16 (9.92, 10.64)	10.45 (10.19, 11.01)	10.56 (10.32, 11.19)	10.65 (10.39, 11.30)
#7	3.35	5.325	9.68 (9.39, 10.11)	9.96 (9.66, 10.50)	10.10 (9.82, 10.71)	10.19 (9.90, 10.84)
#8	3.6	5.55	10.36 (10.05, 10.84)	10.64 (10.26, 11.18)	10.72 (10.35, 11.32)	10.91 (10.51, 11.48)
#9	3.75	5.5	10.86 (10.49, 11.39)	11.14 (10.79, 11.82)	11.28 (10.93, 12.04)	11.34 (10.98, 12.14)
#10	4.1	5.3	11.40 (10.90, 12.04)	11.87 (11.41, 12.68)	12.11 (11.58, 13.03)	12.26 (11.78, 13.23)
#11	4.25	4.75	11.44 (11.11, 12.03)	11.88 (11.56, 12.59)	12.14 (11.78, 12.87)	12.29 (11.92, 13.05)
#12	3.7	3.675	9.69 (9.37, 10.24)	9.89 (9.56, 10.57)	9.93 (9.67, 10.67)	10.02 (9.76, 10.80)
#13	3.65	5.025	11.10 (10.48, 12.07)	11.63 (10.93, 12.88)	11.88 (11.15, 13.30)	12.11 (11.35, 13.68)
#14	4.15	4.8	11.06 (10.65, 11.70)	11.40 (10.99, 12.18)	11.54 (11.14, 12.41)	11.66 (11.26, 12.59)
#15	4.85	4.2	11.31 (10.92, 11.90)	11.74 (11.34, 12.44)	11.95 (11.54, 12.71)	12.07 (11.67, 12.89)
#16	4.45	3.825	10.91 (10.74, 11.38)	11.31 (11.14, 11.83)	11.46 (11.28, 12.02)	11.75 (11.56, 12.33)
#17	3.05	4.775	10.31 (9.65, 11.59)	10.88 (10.03, 12.65)	11.08 (10.18, 13.15)	11.26 (10.35, 13.57)
#18	3.65	4.25	11.63 (11.04, 12.65)	12.00 (11.38, 13.30)	12.18 (11.53, 13.66)	12.36 (11.70, 13.95)
#19	3.55	2.275	7.87 (7.65, 8.33)	8.16 (7.93, 8.70)	8.21 (8.00, 8.83)	8.28 (8.06, 8.91)
#20	3.65	3.575	10.07 (9.53, 11.02)	10.50 (9.94, 11.71)	10.64 (10.05, 12.02)	10.84 (10.23, 12.35)
#21	2.9	4	10.10 (9.32, 11.59)	10.70 (9.87, 12.83)	10.96 (9.94, 13.37)	11.12 (10.21, 13.99)
#22	3	2.9	9.10 (8.57, 10.29)	9.45 (8.87, 11.01)	9.58 (9.00, 11.37)	9.71 (9.09, 11.68)

6. Conclusions and discussions

In general, the threshold selection criterion of Shao et al. (2018a) can be used to assess the extreme significant wave height. However, some return significant wave heights within the stable threshold range may be relatively different from the others, especially for a short return period. For example, at location #12, the return significant wave heights for the return periods of 50-year, 100-year, 150-year and 200-year are 9.59 m, 9.86 m, 9.99 m and 10.06 m, respectively; however, under the criterion of Liang et al. (2019), the corresponding return significant wave heights are 9.69 m, 9.89 m, 9.96 m and 10.05 m, respectively. Benefitting from a diagnostic process of Liang et al. (2019), the return significant wave heights are more stable than those of Shao et al. (2018a). Comparing Table 9 of Shao et al. (2019) with Tables 1 and 2 in this study, the return significant wave heights for the return periods of 50-year, 100-year, 150-year and 200-year are very similar at the same 22 study locations. Both groups of return significant wave heights are reasonable in the SCS. However, the threshold selection criterion in this study is suitable only in a tropical cyclone-dominated area.

Based on a separation within the stable threshold range, a unique threshold can be identified without a subjective definition. Based on further analysis of this distribution, the initial database and characteristics of the tropical cyclones determine a bimodal shape. A fixed distance is used to identify the initial database at the study site. This fixed distance allows some small samples (the corresponding track is far, or the intensity is weak) to be extracted. Thus, other analyses are needed to identify the extreme sample from the sample.

Consequently, the results of this study present a concept linking the assessment of extreme significant wave heights with the characteristics of tropical cyclones in a tropical cyclone-dominated area. The sample at the targeted location is affected by the track and intensity of the tropical cyclone. Future studies are suggested to promote the assessment of extreme significant wave heights in a tropical cyclone. For example, the threshold may be determined directly through a combination of track threshold and intensity threshold.

Acknowledgments

The authors would like to acknowledge the support of the National Science Fund (Grant No. 51679223, 51739010), the 111 Project (Grant No. B14028), Shandong Provincial Natural Science Key Basic Program (Grant No. ZR2017ZA0202) and a grant of the 7th Generation Ultra-Deep-water Drilling Rig Innovation Project.

References

Alves, J.H.G.M. and Young, I.R.: On estimating extreme significant wave heights using combined Geosat, Topex/Poseidon and ERS-1 Altimeter Data, Applied Ocean Research, 25, 167-186, 2003.

Amrutha, M.M., Sanil Kumar, V., Sandhya, K.G., Nair, T.B., and Rathod, J.L.: Wave hindcast studies using SWAN nested in WAVEWATCH III-comparison with measured nearshore buoy data off Karwar, eastern Arabian Sea, Ocean Engineering, 119, 114-124, 2016.

Anoop, T.R., Sanil Kumar, V., Shanas, P.R., and Johnson, G.: Surface wave climatology and its variability in the North Indian Ocean based on ERA-Interim reanalysis, Journal of Atmospheric and Oceanic Technology, 32, 1372-1385, 2015.

Beguería, S.: Uncertainties in partial duration series modelling of extremes related to the choice of the threshold value, Journal of Hydrology, 303, 215-230, 2005.

Beirlant, J., Goegebeur, Y., Segers, J., and Teugels, J.L.: Statistics of extremes: theory and applications, John Wiley & Sons, 2006.

Benetazzo, A., Fedele, F., Carniel, S., Ricchi, A., Bucchignani, E., and Sclavo, M.: Wave climate of the Adriatic Sea: a future scenario simulation, Natural Hazards and Earth System Sciences, 12, 2065-2076, 2012.

Bernardara, P., Mazas, F., Kergadallan, X., and Hamm, L.: A two-step framework for over-threshold modelling of environmental extremes, Natural Hazards and Earth System Sciences, 14, 635, 2014.

Blanchet, J., Touati, J., Lawrence, D., Garavaglia, F., and Paquet, E.: Evaluation of a compound distribution based on weather pattern subsampling for extreme rainfall in Norway, Natural Hazards and Earth System Sciences, 15, 2653-2667, 2015.

Boessenkool, B., Brüger, G., and Heistermann, M.: Effects of sample size on estimation of rainfall extremes at high temperatures, Natural Hazards and Earth System Sciences, 17, 1623-1629, 2017.

Booij, N., Holthuijsen, L.H., and Ris, R.C.: A third-generation wave model for coastal regions: 1. Model description and validation, Journal of Geophysical Research, 104, 7649-7666, 1999.

Caires, S. and Sterl, A.: 100-year return value estimates for ocean wind speed and significant wave, Journal of Climate, 18, 1032-1048, 2005.

Carreau, J. and Bengio, Y.: A hybrid Pareto model for asymmetric fat-tailed data: the univariate case, Extremes, 12, 53-76, 2009.

Chen, X., Wang, K., Zhang, Z., Zeng, Y.D., Zhang, Y., and O'Driscoll, K.: An assessment of wind and wave climate as potential sources of renewable energy in the nearshore Shenzhen coastal zone of the South China Sea, Energy, 134, 789-801, 2017.

Coles, S.: An introduction to statistical modeling of extreme values, Springer Series in Statistics, Springer-Verlag London, London, 2001.

Danielsson, J., de Haan, L., Peng, L., and de Vries, C.G.: Using a bootstrap method to choose the sample fraction in tail index estimation, Journal of Multivariate Analysis, 76, 226-248, 2001.

Eastoe, E.F. and Tawn, J.A.: Statistical models for overdispersion in the frequency of peaks over threshold data for a flow series, Water resources research, 46, 2010.

Embrechts, P., Klüppelberg, C., and Mikosch, T.: Modelling Extremal Events: For Insurance and Finance, Springer, 648, 1997.

Ferreira, J.A. and Guedes Soares, C.: An application of the peaks over threshold method to predict extremes of significant wave height, Journal of Offshore Mechanics and Arctic Engineering, 120(3), 165-176, 1998.

Ferreira, A., de Haan, L., and Peng, L.: On optimising the estimation of high quantiles of a probability distribution, Statistics, 37(5), 401-434, 2003.

Gao, H.J., Wang, L.Q., Liang, B.C., and Pan, X.Y.: Estimation of Extreme Significant Wave Heights in the Yellow Sea, China, The 28th International Ocean and Polar Engineering Conference, International Society of Offshore and Polar Engineers, 387-391, 2018.

Goda, Y., Konagaya, O., Takeshita, N., Hitomi, H., and Nagai, T.: Population distribution of extreme significant wave heights estimated through regional analysis, International Conference on Coastal Engineering, 276, 1078-1091, 2001.

Godoi, V.A., Bryan, K.R., Stephens, S.A., and Gorman, R.M.: Extreme waves in New Zealand waters, Ocean Modelling, 117, 97-110, 2017.

Goegebeur, Y., Beirlant, J., and de Wet, T.: Linking Pareto-tail kernel goodness-of-fit statistics with tail index at optimal threshold and second order estimation, Revstat, 6(1), 51-69, 2008.

Hill, B.M.: A simple general approach to inference about the tail of a distribution, the Annals of Statistics, 3(5), 1163-1174, 1975.

Hithin, N.K., Sanil Kumar, V., and Shanas, P.R.: Trends of wave height and period in the Central Arabian Sea from 1996 to 2012: a study based on satellite altimeter data, Ocean Engineering, 108, 416-425, 2015.

Kapelonis, Z.G., Gavriliadis, P.N., and Athanassoulis, G.A.: Extreme value analysis of dynamical wave climate projections in the Mediterranean Sea, Procedia Computer Science, 66, 210-219, 2015.

Lerma, A.N., Bulteau, T., Lecacheux, S., and Idier, D.: Spatial variability of extreme significant wave height along the Atlantic and channel French coast, Ocean Engineering, 97, 175-185, 2015.

Li, J., Pan, S., Chen, Y., Fan, Y.M., and Pan, Y.: Numerical estimation of extreme waves and surges over the northwest Pacific Ocean, Ocean Engineering, 153, 225-241, 2018.

Liang, B.C., Shao, Z.X., Li, H.J., Shao, M., and Lee, D.Y.: An automated threshold selection method based on the characteristic of extrapolated significant wave heights, Coastal Engineering, 144, 22-32, 2019.

Lucas, C., Muraleedharan, G., and Soares, C.G.: Regional frequency analysis of extreme waves in a coastal area, Coastal Engineering, 126, 81-95, 2017.

MacDonald, A., Scarrott, C.J., Lee, D., Darlow, B., Reale, M., and Russell, G.: A flexible extreme value mixture model, Computational Statistics & Data Analysis, 55(6), 2137-2157, 2011.

Martucci, G., Carniel, S., Chiggiato, J., Sclavo, M., Lionello, P., and Galati, M.B.: Statistical trend analysis and extreme distribution of significant wave height from 1958 to 1999-an application to the Italian Seas, Ocean Science, 6, 525-538, 2010.

Mazas, F., and Hamm, L.: Amulti-distribution approach to POT methods for determining extreme significant wave heights, Coastal Engineering, 58(5), 385-394, 2011.

Mirzaei, A., Tangang, F., and Juneng, L.: Wave energy potential assessment in the central and southern regions of the South China Sea, Renewable Energy, 80, 454-470, 2015.

Mortlock, T.R., Goodwin, I.D., and Turner, I.L.: Nearshore SWAN model sensitivities to measured and modelled offshore wave scenarios at an embayed beach compartment, NSW, Australia, Australian Journal of Civil Engineering, 12(1), 67-82, 2014.

Mortlock, T.R., and Goodwin, I.D.: Directional wave climate and power variability along the Southeast Australian shelf, Continental Shelf Research, 98, 36-53, 2015.

Mortlock, T.R., and Goodwin, I.D.: Impacts of enhanced central Pacific ENSO on wave climate and headland-bay beach morphology, Continental Shelf Research, 120, 14-25, 2016.

Mortlock, T.R., Goodwin, I.D., McAneney, J.K., and Roche, K.: The June 2016 Australian East Coast Low: Importance of Wave Direction for Coastal Erosion Assessment, Water, 9(2), 121, 2017.

Mortlock, T.R., Metters, D., Soderholm, J., Maher, J., Lee, S.B., Boughton, G., Stewart, N., Zavadil, E., and Goodwin, I.D.: Extreme water levels, waves and coastal impacts during a severe tropical cyclone in Northeast Australia: a case study for cross-sector data sharing, Natural Hazards and Earth System Sciences, 1-37, 2018.

Muhammed Naseef, T. and Sanil Kumar, V.: Variations in return value estimate of ocean surface waves-a study based on measured buoy data and ERA-Interim reanalysis data, Natural Hazards and Earth System Sciences, 17(10), 1763-1778, 2017.

Muraleedharan, G., Lucas, C., and Soares, C.G.: Regression quantile models for estimating trends in extreme significant wave heights, Ocean Engineering, 118, 204-215, 2016.

Neves, C. and Alves, M.I.F.: Reiss and Thomas' automatic selection of the number of extremes, Computational Statistics & Data Analysis, 47(4), 689-704, 2004.

Northrop, P.J. and Coleman, C.L.: Improved threshold diagnostic plots for extreme value analyses, Extremes, 17(2), 289-303, 2014.

Northrop, P.J., Attalides, N., and Jonathan, P.: Cross‐validatory extreme value threshold selection and uncertainty with application to ocean storm severity, Journal of the Royal Statistical Society: Series C (Applied Statistics), 66(1), 93-120, 2017.

Ojeda, E. and Guillén, J.: Shoreline variability of Barcelona city beaches in response to storms and artificial nourishment (2001-2003), Coastal Dynamics 2005: State of the Practice, 1-11, 2006.

Ojeda, E. and Guillén, J.: Shoreline dynamics and beach rotation of artificial embayed beaches, Marine Geology, 253(1-2), 51-62, 2008.

Ojeda, E., Guillén, J., and Ribas, F.: The morphodynamic responses of artificial embayed beaches to storm events, Advances in Geosciences, 26, 99-103, 2010.

Ojeda, E., Guillén, J., and Ribas, F.: Dynamics of single-barred embayed beaches, Marine Geology, 280(1-4), 76-90, 2011.

Ojeda, E., Appendini, C.M., and Mendoza, E.T.: Storm-wave trends in Mexican waters of the Gulf of Mexico and Caribbean Sea, Natural Hazards and Earth System Sciences, 17(8), 1305-1317, 2017.

Petrov, V., Guedes Soares, C., and Gotovac, H.: Prediction of extreme significant wave heights using maximum entropy, Coastal Engineering, 74, 1-10, 2013.

Pickands, J.: Statistical inference using extreme order statistics, the Annals of Statistics, 3, 119-131, 1975.

Reiss, R.D. and Thomas, M.: Statistical analysis of extreme values, Basel: Birkhäuser, 2007.

Samayam, S., Laface, V., Annamalaisamy, S.S., Arena, F., Vallam, S., and Gavrilovich, P.V.: Assessment of reliability of extreme wave height prediction models, Natural Hazards and Earth System Sciences, 17(3), 409-421, 2017.

Sánchez-Arcilla, A., Gomez Aguar, J., Egozcue, J.J., Ortego, M.R., Galiatsatou, P., and Prinos, P.: Extremes from scarce data: the role of Bayesian and scaling techniques in reducing uncertainty, Journal of Hydraulic Research, 46(S2), 224-234, 2017.

Sanil Kumar, V. and Anoop, T.R.: Spatial and temporal variations of wave height in shelf seas around India, Natural Hazards, 78(3), 1693-1706, 2015.

Sanil Kumar, V., Joseph, J., Amrutha, M.M., Jena, B.K., Sivakholundu, K.M., and Dubhashi, K.K.: Seasonal and interannual changes of significant wave height in shelf seas around India during 1998-2012 based on wave hindcast, Ocean Engineering, 151, 127-140, 2018.

Scarrott, C. and MacDonald, A.: A review of extreme value threshold estimation and uncertainty quantification, Statistical Journal, 10(1), 33-60, 2012.

Schendel, T. and Thongwichian, R.: Confidence intervals for return levels for the peaks-over-threshold approach, Advances in Water Resources, 99, 53-59, 2017.

Shao, Z.X., Liang, B.C., Pan, X.Y., and Gao, H.J.: Analysis of Extreme Waves with Tropical Cyclone Wave Hindcast Data, The 27th International Ocean and Polar Engineering Conference, International Society of Offshore and Polar Engineers, 30-33, 2017.

Shao, Z.X., Liang, B.C., Li, H.J., and Lee, D.Y.: Study of sampling methods for assessment of extreme significant wave heights in the South China Sea, Ocean Engineering, 168, 173-184, 2018a.

Shao, Z.X., Liang, B.C., Li, H.J., Wu, G.X., and W, Z.H.: Blended wind fields for wave modeling of tropical cyclones in the South China Sea and East China Sea, Applied Ocean Research, 71, 20-33, 2018b.

Soares, C.G. and Scotto, M.G.: Application of the r largest-order statistics for long-term predictions of significant wave height, Coastal Engineering, 51(5-6), 387-394, 2004.

Sobradelo, R., Martí, J., Mendoza-Rosas, A.T., and Gómez, G.: Volcanic hazard assessment for the Canary Islands (Spain) using extreme value theory, Natural Hazards and Earth System Sciences, 11(10), 2741-2753, 2011.

Solari, S. and Alonso, R.: A new methodology for extreme waves analysis based on weather-patterns classification methods, Coastal Engineering Proceedings, 1(35), 23, 2017.

Solari, S., Egüen, M., Polo, M.J., and Losada, M.Á.: Peaks Over Threshold (POT): A methodology for automatic threshold estimation using goodness of fit p-value, Water Resources Research, 53(4), 2833-2849, 2017.

Sulis, A., Cozza, R., and Annis, A.: Extreme wave analysis methods in the gulf of Cagliari (South Sardinia, Italy), Ocean & Coastal Management, 140, 79-87, 2017.

Tawn, J.A.: An extreme-value theory model for dependent observations, Journal of Hydrology, 101(1-4), 227-250, 1988.

Vanem, E.: Non-stationary extreme value models to account for trends and shifts in the extreme wave climate due to climate change, Applied Ocean Research, 52, 201-211, 2015a.

Vanem, E.: Uncertainties in extreme value modelling of wave data in a climate change perspective, Journal of Ocean Engineering and Marine Energy, 1(4), 339-359, 2015b.

Viselli, A.M., Forristall, G.Z., Pearce, B.R., and Dagher, H.J.: Estimation of extreme wave and wind design parameters for offshore wind turbines in the Gulf of Maine using a POT method, Ocean Engineering, 104, 649-658, 2015.

Wang, L.Q., Liang, B.C., Li, H.J.: A new non-parametric correction model and its applications to hindcasting wave data, Ocean Engineering, 132, 11-24, 2017.

Wang, Z., Duan, C., and Dong, S.: Long-term wind and wave energy resource assessment in the South China sea based on 30-year hindcast data, Ocean Engineering, 163, 58-75, 2018.

Xiao, L., Lu, H., Tao, L., and Yang, L.J.: LH-moment estimation for statistical analysis on the wave crest distributions of a deepwater spar platform model test, Marine Structures, 52, 15-33, 2017.

Yaakob, O., Hashim, F.E., Omar, K.M., Din, A.H.M., and Koh, K.K.: Satellite-based wave data and wave energy resource assessment for South China Sea, Renewable Energy, 88, 359-371, 2016.

You, Z.J.: Extrapolation of historical coastal storm wave data with best-fit distribution function, Australian Journal of Civil Engineering, 9, 73-82, 2011.

You, Z.J. and Callaghan, D.: Discussion of "Modelling significant wave height distributions with quantile functions for estimation of extreme significant wave heights" [Ocean Eng. 54 (2012) 119–131], Ocean Engineering, 70, 208-210, 2013.

Zheng, C.W., Zhuang, H., Li, X., and Li, X.Q.: Wind energy and wave energy resources assessment in the East China Sea and South China Sea, Science China Technological Sciences, 55(1), 163-173, 2012.

Zheng, C.W., Pan, J., Tan, Y.K., Gao, Z.S., Rui, Z.F., and Chen, C.H.: The seasonal variations in the significant wave height and sea surface wind speed of the China's seas, Acta Oceanologica Sinica, 34(9), 58-64, 2015.